Quantum Network Tomography with Multi-party State Distribution

Matheus Guedes de Andrade¹, Jaime Diaz², Jake Navas², Saikat Guha³, Inès Montaño², Brian Smith⁴, Michael Raymer⁴, and Don Towsley¹

¹College of Information and Computer Science, University of Massachusetts Amherst ²Department of Applied Physics and Materials Science, Northern Arizona University ³College of Optical Sciences, University of Arizona ⁴Department of Physics, University of Oregon

Abstract—The fragile nature of quantum information makes it practically impossible to completely isolate a quantum state from noise under quantum channel transmissions. Quantum networks are complex systems formed by the interconnection of quantum processing devices through quantum channels. In this context, characterizing how channels introduce noise in transmitted quantum states is of paramount importance. Precise descriptions of the error distributions introduced by nonunitary quantum channels can inform quantum error correction protocols to tailor operations for the particular error model. In addition, characterizing such errors by monitoring the network with end-to-end measurements enables end-nodes to infer the status of network links. In this work, we address the end-to-end characterization of quantum channels in a quantum network by introducing the problem of Quantum Network Tomography. The solution for this problem is an estimator for parameters that define a Kraus decomposition for all quantum channels in the network, using measurements performed exclusively in the endnodes. We study this problem in detail for the case of arbitrary star quantum networks with quantum channels described by a single Pauli operator, like bit-flip quantum channels. We provide solutions for such networks with polynomial sample complexity. Our solutions provide evidence that pre-shared entanglement brings advantages for estimation in terms of the identifiability of parameters.

I. INTRODUCTION

Quantum networks are communication systems formed by the interconnection of quantum processors with channels that enable the communication of quantum information [1]–[4]. They extend the capabilities of quantum computers, augmenting the computing power of interconnected quantum processors with distributed quantum computing [5], [6], and enable novel applications such as quantum key distribution [7] and entanglement-enabled very-long-baseline interferometric telescopes [8]. As with any quantum processing system, noise is inherent to quantum networks due to the fragile nature of quantum information.

In networked systems, noise arises both in the communication of quantum information through channels and in the quantum operations performed by the nodes. The diverse ecosystem of physical platforms for qubit implementations, as well as the communication media used, have drastic impacts on errors introduced during communication, such that the

development of technologies to transduce quantum information is critical [9], [10]. With respect to communication, quantum information encoded in photons is subject to different errors when propagated through optical fiber and through freespace [11]. Therefore, characterizing communication errors is central in a heterogeneous quantum network that includes satellites and optical fibers. For instance, quantum error correction processes [12] and entanglement purification methods [13] can benefit from a precise description of error models to improve efficiency.

In the context of characterizing quantum systems, the theory of quantum estimation determines the fundamental limits to what can be inferred from measurements and the efficiency of realizable estimators [14], [15]. Thus, quantum estimation is the key tool to describe errors introduced by noise in communication in a quantum network. Quantum Tomography refers to a set of quantum estimation methods for inferring the description of quantum systems [16]. Quantum State Tomography [17] and Quantum Process Tomography [18] refer to methods for describing quantum states and quantum evolution processes, respectively. Hence, one could attempt to characterize errors in a quantum network using standard quantum tomography methods, where the network would be treated as a black-box and probed through the transmission of quantum states which would be measured to estimate the behavior of the entire network.

Unfortunately, such methods are not directly applicable if one wants to characterize the behavior of individual network links through measurements at only end-nodes. Consequently, investigating methods that use prior knowledge of the network topology and the form of errors that arise from noise introduced by quantum channel transmissions brings a new perspective to such a tomography problem.

Exploiting prior knowledge to characterize channels in classical networks has been previously investigated and motivated the development of classical Network Tomography [19], [20]. Classical Network Tomography refers to a set of methods that aim to estimate the status of network links through end-to-end measurements. The key idea is to transmit packets among end-nodes in the network with the necessary meta-information to measure classical quantities such as transmission delay and packet loss. In the classical network scenario, tomography

methods that use both unicast and multicast communication were proposed. Interestingly, link correlations introduced by multicast communication in packet loss were exploited to provide estimators for the loss probability per link in multicast trees from end-to-end measurements [21], [22].

A. Contributions

The goal of this work is to bridge quantum tomography with classical network tomography by introducing the problem of Quantum Network Tomography. Our contributions are as follows.

- We formally define the problem of Quantum Network Tomography for generic quantum networks as the estimation
 of parameters determining operator-sum representations
 for all quantum channels in a network. The definition
 captures end-to-end parameter estimation, including parameters internal to the network, considering estimators
 based on measurements performed exclusively in the endnodes.
- We define a generic multi-party state distribution process for the network tomography of arbitrary trees.
- We solve quantum network tomography problems in star networks using the above multi-party state distribution process. In particular, we focus on the case of random unitary channels characterized by a single Pauli operator, such as a bit-flip channel, and provide estimators for network parameters with polynomial sample complexity. Our estimators attain the Quantum Cramèr-Rao bound and provide evidence that, even for single Pauli channels, pre-shared entanglement may bring advantages for estimation in terms of parameter identifiability.
- Finally, we compare the performance of our estimators numerically for a four-node star network.

The remainder of this article is structured as follows. In Section II, we provide the necessary mathematical background to discuss our results. We define the problem of quantum network tomography in Section III and describe the multiparty state distribution process in Section IV. We report our results for the tomography problem in the case of star networks with channels described by a single Pauli operator in Section V. Finally, we discuss our results and present concluding remarks in Section VI.

II. DEFINING QUANTUM NETWORK TOMOGRAPHY

In this work, we consider quantum networks to be systems formed by the interconnection of quantum processing devices with quantum channels that allow for communication of quantum information. We do not assume any particular physical implementation of the underlying quantum channels, nor any choice of qubit platform. In addition, we use the term quantum processing device, or quantum processor, to abstract quantum computers, routers, switches and repeaters.

We represent a quantum network as a graph G=(V,E), where the nodes in V denote the quantum processors and the edges in E represent the quantum channels interconnecting the nodes. In addition, the node set is partitioned as $V=V_E\cup V_I$,

where V_E and V_I determine the sets of end and intermediate nodes in the network.

Quantum processors are assumed capable of performing generic, unitary quantum operations on its quantum registers and perfect quantum measurements. This assumption implies that the only source of error in the network comes from the transmission of quantum information through the channels. Despite being unrealistic, assuming perfect quantum operations in the nodes is the initial step for the investigation of the estimation problems within the scope of this article.

A star quantum network is a system consisting of one intermediate node interconnecting n end-nodes. In this particular case, we have |V|=n+1, |E|=n and each end-node identifies one edge of the star. For simplicity, we label the intermediate node as node n and edge (v,n) as the v-th edge, for $v \in \{0,1,\ldots,n-1\}$, i.e $V_E = \{0,1,\ldots,n-1\}$ and $V_I = \{n\}$.

In what concerns notation, we use \mathcal{H}^K to represent the Hilbert space with dimension 2^K formed by K qubits and \mathcal{D}^K to represent the space of density matrices of K-qubit systems. The Greenberger-Horne-Zeillinger (GHZ) basis is formed by maximally entangled states and generalizes the Bell basis to multiple qubits. Let $s=s_0\dots s_{n-2}\in\{0,1\}^{n-2}$ be a binary string of length (n-1) and $b\in\{0,1\}$ be a single bit. We represent states in the n-qubit GHZ basis as

$$\left|\Phi_s^b\right\rangle = \frac{\left|0s_0\dots s_{n-1}\right\rangle + (-1)^b \left|1\overline{s_0\dots s_{n-1}}\right\rangle}{\sqrt{2}},\qquad(1)$$

where $\overline{s_k}$ is the logical negation of bit s_k . For simplicity, we often use a single variable s to refer to a binary string, with \overline{s} representing its bit-wise logical negation. As an example, the standard three-qubit GHZ state $(|000\rangle + |111\rangle)/\sqrt{2}$ is expressed as $|\Phi^0_{00}\rangle$ in (1). GHZ-basis projectors are defined as $\Phi^b_s = |\Phi^b_s\rangle\langle\Phi^b_s|$. We use the standard notation of [.,.]:[A,B] = AB - BA and $\{.,.\}:\{A,B\} = AB + BA$ to respectively denote the commutator and anti-commutator of operators.

A. Quantum channels in the network

The edges in |E| represent Completely Positive Trace-Preserving (CPTP) single-qubit maps, which implies that qubits are never lost after channel transformations. We assume that, for every edge $e=(u,v)\in E$, the quantum channel $\mathcal{E}_v:\mathcal{D}^2\to\mathcal{D}^2$ that interconnects nodes u and v corresponds to the mapping

$$\mathcal{E}_e(\rho) = \sum_{k=0}^{d_e-1} K_{ek} \rho K_{ek}^{\dagger} \tag{2}$$

where $\{K_{ek}\}$ is a set of Kraus operators for link e and ρ is a one-qubit density matrix. In the case of random unitary quantum channels, the Kraus operators become $K_{ek} = \sqrt{\theta_{ek}} U_{ek}$, where U_{ek} is a unitary operator and $\{\theta_{ek}\}$ are probabilities with $\sum_k \theta_{ek} = 1$.

The generalized depolarizing channel is a random unitary channel with Kraus operators described by Pauli operators, having an operator-sum representation of form

$$\mathcal{E}_e(\rho) = \sum_{k=0}^3 \theta_{ek} \sigma_k \rho \sigma_k, \tag{3}$$

where $\theta_e \in \mathbb{R}^4$ and $\{\sigma_k\}$ denote the set of Pauli operators, with $\sigma_0 = I$. When channels are described by a single Pauli operator, (3) reduces to

$$\mathcal{E}_e(\rho) = \theta_e \rho + (1 - \theta_e) \sigma \rho \sigma \tag{4}$$

where $\sigma \in \{X, Y, Z\}$ is one of the Pauli operators and the channel is described by a single parameter $\theta_e \in \mathbb{R}$.

B. Quantum estimation

Quantum estimation theory addresses how measurements can be used to obtain information from quantum systems. There are three fundamental aspects of any quantum estimation problem [15]. Assume that it is of interest to estimate a parameter vector θ . First, it is necessary to obtain a quantum state ensemble ρ that is parameterized by θ , what is normally referred to as parameterization. Second, it is necessary to measure ρ to obtain measurement statistics. Finally, we need to design estimators for θ based on measurement outcomes.

Suppose that we are given a parameterized state ensemble of N qubits. In particular, let $\rho:\mathbb{R}^M\to\mathcal{D}^N$ denote the density matrix of the system that depends on a parameter vector $\theta\in\mathbb{R}^M$ as

$$\rho(\theta) = \sum_{k=0}^{R-1} \lambda_k(\theta) \Lambda_k(\theta), \tag{5}$$

where R is the rank of $\rho(\theta)$, $\{\Lambda_k\}$ is the set of projectors for the eigenspace of $\rho(\theta)$ and $\lambda_k: \mathbb{R}^M \to \mathbb{R}$ are θ -dependent probability values for which $\sum_k \lambda_k(\theta) = 1$. We are interested in the following quantum estimation problem.

Problem 1 (Quantum parameter estimation). Find an estimator $\hat{\theta}$ for θ from measurements performed in an ensemble of states prepared following the density matrix $\rho(\theta)$.

The measurement statistics used to describe $\hat{\theta}$ will depend on the measurement performed. For any set of *Positive Operator-Valued Measure* (POVM) elements $\{\Pi_l\}$, the probability of having outcome l as a measurement result is

$$p_{\theta}(\Pi_l) = \sum_{k=0}^{R-1} \lambda_k(\theta) \operatorname{Tr}(\Lambda_k(\theta)\Pi_l).$$
 (6)

Note that POVM elements can act on any subset of the N qubits in the system. Thus, if the form of p_{θ} is known, measuring an ensemble of states described by $\rho(\theta)$ with $\{\Pi_l\}$ yields estimators $\hat{p}_{\theta}(\Pi_l) \in \mathbb{R}^+$ for $p_{\theta}(\Pi_l)$, and $\hat{\theta}$ can be obtained by solving the inverse problem

$$p_{\hat{\theta}}(\Pi_l) = \hat{p}_{\theta}(\Pi_l), \text{ for all } l,$$
 (7)

where $p_{\hat{\theta}}(\Pi_l)$ is the analytical description in the r.h.s of (6). There are two aspects of such an estimation problem. First, the number of equations obtained is the number of

POVM elements. For projective measurements, the number of equations grows as $\mathcal{O}(2^N)$ because of the completeness relation. Second, the dependence of $p_{\theta}(\Pi_l)$ on θ does not guarantee that the inverse problem in (7) has a unique solution.

C. Estimation efficiency

In general, different parametrization processes provide mixed states described by different density matrices, which leads to distinct estimators $\hat{\theta}$ for θ . In addition, different POVMs yield distinct estimators for the same density matrix $\rho(\theta)$. Thus, we analyze the efficiency of different estimators for Problem 1 with two metrics of interest: the *identifiability* of $\hat{\theta}$ and the *Quantum Fisher Information Matrix* (QFIM) for θ [15].

We say that an estimator $\hat{\theta}$ identifies θ if it determines a unique value for θ from a sequence of observations. In the case of (7), $\hat{\theta}$ identifies the parameters if it is the unique solution to the inverse problem.

The QFIM \mathcal{F} of a density matrix $\rho(\theta)$ [14] is a positive semi-definite real matrix with entries

$$\mathcal{F}_{jk} = \frac{1}{2} \operatorname{Tr}(\rho \{L_j, L_k\}), \tag{8}$$

where L_k is the Symmetric Logarithmic Derivative operator (SLD) of $\rho(\theta)$ with respect to θ_j given by the differential matrix equation

$$\frac{\partial \rho}{\partial \theta_j} = \frac{1}{2} (L_j \rho + \rho L_j). \tag{9}$$

The diagonal entry \mathcal{F}_{jj} is the *Quantum Fisher Information* (QFI) for parameter θ_j . The QFIM yields the *Quantum Cramèr-Rao bound* (QCRB) for multi-parameter estimation, which is a lower bound on the covariance matrix of any estimates based on statistics generated by any POVM [15]. An estimator that reaches the QCRB for the joint estimation of θ is attainable if, and only if L_j and L_k commute for all pairs θ_j , θ_k [15].

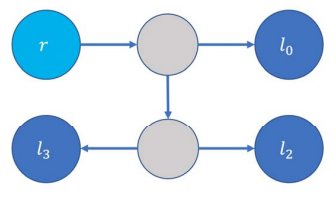
Furthermore, consider the following simple theorem.

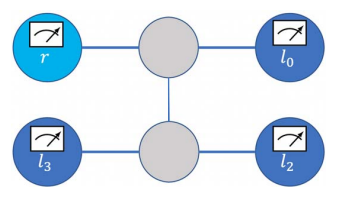
Theorem 1. If $\rho(\theta) = \sum_k \lambda_k(\theta) \Lambda_k$ is diagonalized by a set of θ -independent projectors $\{\Lambda_k\}$, then $\{\Lambda_k\}$ diagonalizes L_j , for all j.

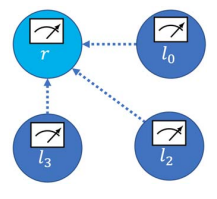
Proof. Under the assumption that $\Lambda_k(\theta) = \Lambda_k$, $\rho(\theta) = \sum_k \lambda_k(\theta) \Lambda_k$ and $\frac{\partial \rho(\theta)}{\partial \theta_j} = \sum_k \frac{\partial \lambda(\theta)}{\partial \theta_j} \Lambda_k$ for all j. Thus, by taking the ansatz $L_j = \sum_k l_{jk} \Lambda_k$, one verifies that (9) is solved with $l_{jk} = \frac{\partial \lambda(\theta)}{\partial \theta_j} \frac{1}{\lambda(\theta)}$, for all j.

When Theorem 1 is valid, L_i and L_j commute for all i,j and an estimator $\hat{\theta}$ from projective measurements on the $\{\Lambda_k\}$ basis is asymptotically optimal given $\rho(\theta)$. Plugging the description for L_i from Theorem 1 in (8) yields

$$\mathcal{F}_{ab} = \sum_{k} \frac{1}{\lambda_k} \frac{\partial \lambda_k}{\partial \theta_a} \frac{\partial \lambda_k}{\partial \theta_b}.$$
 (10)







(a) State distribution.

(b) End-to-end measurements.

(c) Collection and estimation.

Fig. 1: Quantum network tomography on trees. The tree shown is formed by two intermediate nodes and each link is described by a Kraus decomposition of known form (Equation 11). The goal is to estimate the probabilities describing each link in the tree. (a) A mixed state $\rho(\theta)$ is distributed from the root r towards the leaves l_j . To perform distribution, the root and the intermediate nodes (gray circles) transmit a qubit state to its neighbors following arrow direction. (b) When all leaves receive qubits, measurements are performed to obtain classical data for estimation. (c) Finally, end-nodes transmit the classical data from measurements to a single node in the network, represented here by the root node, for estimation to be performed.

III. QUANTUM NETWORK TOMOGRAPHY

In this section we formally define the problem of quantum network tomography. We begin by describing the problem of quantum link tomography, which naturally leads to the definition of the network version. Consider the simplest nontrivial network system formed by two end-nodes u and v connected by an edge e=(u,v) representing the quantum channel \mathcal{E}_e following (2). The link tomography problem refers to quantum process tomography of \mathcal{E}_e . In its most general form, one does not assume any knowledge of \mathcal{E}_e and its solution is a description of a set of Kraus operators $\{K_{ek}\}$ that characterize \mathcal{E}_e [18].

This general problem is difficult, since the Kraus operators must be characterized from measurements, treating \mathcal{E}_e as a black-box. We simplify this problem by assuming that a parametric description of (2) of the form

$$\mathcal{E}_e(\rho) = \sum_k K_{ek}(\theta) \, \rho \, K_{ek}^{\dagger}(\theta), \tag{11}$$

is known and focus on estimation of the parameter θ . Thus, the formal definition of the channel tomography problem of interest is as follows.

Problem 2 (Quantum Link Tomography). Given a set of M Kraus operators $\{K_k\}_e$ for which the quantum channel \mathcal{E}_e represented by link e has the form given in (11), estimate a parameter vector $\hat{\theta}_e \in \mathbb{R}^M$ that characterizes \mathcal{E}_e .

The link tomography problem is an instance of Problem 1 since, in order to estimate the probability vector, it is necessary to use channel \mathcal{E}_e to prepare and measure an ensemble of mixed states that depends on θ to obtain statistics for estimation. In this case, u and v are end-nodes and can perform arbitrary measurements on the ensemble, share the classical results of the measurements and compute $\hat{\theta}_e$.

The quantum network tomography problem, which is depicted in Figure 1 for trees, extends the channel problem to networks with the caveat that only end-nodes can contribute information for estimation. We now present the formal definition of the quantum network tomography problem, which is one of the main contributions of this article.

Problem 3 (Quantum Network Tomography). Given a quantum network G, with nodes partitioned into disjoint sets V_E

and V_I and a set of Kraus operators $\{K_k\}_e$ for each $e \in E$, find an estimator $\hat{\theta}_e$ for the parameter vector θ_e characterizing \mathcal{E}_e as in (11), for all $e \in E$, using measurement statistics from nodes in V_E exclusively.

Problem 3 generalizes 2 to generic networks adding the restriction that measurement observations used for estimation must come from end-nodes. If such a restriction is dropped, the network problem reduces to the link problem and the most efficient way to obtain estimators is to solve Problem 2 independently for all links in the network. When the restriction is considered, joint estimation of the channel parameters must be carried out in the general case. The joint estimation reflects the fact that links must be jointly used to prepare an ensemble $\rho(\theta)$ of states that can be measured by the end-nodes to provide statistics for estimation.

IV. PARAMETERIZATION AND STATE DISTRIBUTION

We now propose a family of parameterization processes that cast Problem 3 into an instance of Problem 1 for a network with a tree topology as depicted in Figure 1. A tree T=(V,E) is a connected graph with no cycles. Tree tomography is interesting since trees are connected graphs with minimum edge density |E|/|V| when |V| is fixed, reducing the number of parameters to be simultaneously estimated. Furthermore, all the links of a network can be covered with multiple trees and characterized through tree tomography through such a covering, although we focus on quantum network tomography of single trees.

In principle, the preparation of $\rho(\theta)$ must target qubits in the end-nodes for measurements to be performed. Such a preparation must use the channels in the network in order to make the ensemble dependent on θ . Regardless of how channels are used to prepare the ensemble, the parameterization process can be expressed as an abstract, multi-qubit quantum channel \mathcal{N}_{θ} acting on a locally-prepared ensemble ρ_0 as $\rho(\theta) = \mathcal{N}_{\theta}(\rho_0)$. In our terminology, a locally-prepared state is any state that is separable with respect to the nodes of the network such that ρ_0 follows

$$\rho_0 = \bigotimes_{v \in V} \rho_{0v},\tag{12}$$

where ρ_{0v} is a multi-qubit state located in a quantum register in node v. The key aspect of quantum network tomography is that both ρ_0 and \mathcal{N}_{θ} are allowed to be chosen as part of the problem's solution.

We describe the abstract quantum channel \mathcal{N}_{θ} , and hence the parameterization process, as a network state distribution process. The state distribution problem refers to the preparation of generic quantum states across target end-nodes, using channels and intermediate nodes to propagate entanglement. In this setting, nodes start with a state that follows (12), which is progressively transformed through local operations and quantum state transmissions across channels. State distribution is a natural approach to define \mathcal{N}_{θ} because qubits transmitted across a link e evolve according to \mathcal{E}_{e} and, thus, can be used to incorporate $\{\theta_{ek}\}$ into the density matrix describing the distributed state. This process yields a quantum channel \mathcal{N}_{θ} that is a composition of $\{\mathcal{E}_{e}\}$ for all $e \in E$ used for distribution.

We propose a distribution process for trees (Algorithm 1) to distribute quantum states across the network with properties tailored for tomography. Since trees have no cycles, there exists exactly one path interconnecting any two nodes in the network. Moreover, the process uses each link in the network to transmit a qubit among neighboring nodes exactly once. Such a process is very general in the sense that it captures any quantum state distribution operation across a tree under the restriction that a single qubit is transmitted between the nodes for distribution.

Thus, consider the following definitions. Let T = (V, E)be a tree rooted at node r. The height function $h: V \to \mathbb{Z}^+$ is defined such that h(v) is the hop-distance of the path connecting v and r in T. Note that h(r) = 0. Let the predecessor of v be the neighbor P_v of v with $h(P_v) = h(v) - 1$, which is not defined for r. Let the successor set of v be $S_v = \{u : (v, u) \in E \text{ and } u \neq P_v\}, v \in T. \text{ A leaf } v$ of T is a node with no successor, $S_v = \emptyset$. Let the set $L_T = \{v : S_v = \emptyset\}$ denote the set of leaves of T and $H(k) = \{v : h(v) = k\}$ the set of all nodes of T with height h. Furthermore, let \mathcal{C} denote the description of a quantum circuit applied in the nodes of the network such that C_v is a generic, multi-qubit circuit applied in node v. Given the circuit C_v , let n_v denote the number of qubits in C_v . Let $\eta: E \to \mathbb{Z}^+$ be a function determining the index of qubits to be transmitted between neighbors. $\eta(u,v)$ determines the index of the output qubit from C_u to be transmitted from u to v after C_u is performed. Finally, let $|0_n\rangle\langle 0_n|$ denote the pure state $|0\rangle\langle 0|^{\otimes n}$.

The process in Algorithm 1 is understood as follows. The inputs are the rooted tree T, a quantum circuit description $\mathcal C$ and a qubit index function η . In order to simplify the process description, we assume that the initial local state ρ_0 is encoded in the circuit description $\mathcal C$, such that all nodes start with registers prepared in a pure state of form $|0_n\rangle\langle 0_n|$. The process begins with the root node executing $\mathcal C_r$. Note that, since the root has no predecessor, line 3 has no effect for v=r. Then, the root sends one qubit from the output of $\mathcal C_r(|0_{n_r}\rangle\langle 0_{n_r}|)$ to each one of its successors, and keeps $n_r - |S_r|$ qubits in memory. The function $\eta(r,v)$ specifies which of the n_r qubit

is transmitted from r to v, for all neighbors v of r. Whenever node v receives a qubit, the channel \mathcal{E}_{P_v} interconnecting P_v and v transforms the initially transmitted state. Thus, node v applies the quantum circuit \mathcal{C}_v with n_v local qubits in state $|0_{n_v}\rangle\langle 0_{n_v}|$ and with the qubit that went through \mathcal{E}_{P_v} as input. The node proceeds by transmitting one qubit to each one of its successors following η , again keeping $n_v - |S_v|$ qubits in memory. The process terminates when each leaf receives a qubit state from its predecessor.

The generality of the process described in Algorithm 1 stems from the freedom of defining both $\mathcal C$ and η , although it should be clear from its description that the distributed mixed state depends on θ_{ek} , for all $e \in E$, as long as $\mathcal C_v$ contains non-separable quantum operations. There exists a direct mapping determining the form of $\mathcal N_\theta$ from T, $\mathcal C$ and η , although writing the mathematical form for the general case is lengthy. In the remainder of this article, we consider distribution circuits where no qubits remain in intermediate nodes after distribution, where each leaf of receives one qubit and where the root may or may not keep one qubit in memory after transmitting to its descendants. Furthermore, we focus on the description of $\rho(\theta)$ directly rather than explicitly writing $\mathcal N_\theta$.

V. TOMOGRAPHY IN STAR NETWORKS

In this section we apply Algorithm 1 to solve tomography problems in star quantum networks. The star graph is a simple type of tree for which we can observe the workings of the distribution process and study tomography in detail. We consider the bi-partition of the nodes defined in Section II, where all leaves are end-nodes and the intermediate node is the center node, as depicted in Figure 2. This bi-partition of nodes is interesting because the distance between end-nodes is always two. Thus, the star is a minimal set-up with a single intermediate node that allows us to investigate the effects of restricting measurements for estimation to end-nodes.

In addition, we simplify the problem further by considering a scenario where every link is described by a single Pauli operator following (4). This simplification helps both the description and evaluation of estimators without rendering the problem trivial. Such class of channels suffices to demonstrate the difficulty of performing tomography in a network and builds intuition on how to approach the problem for more complex channels like the generic depolarizing channel in (3), which is described by all Pauli operators. The formal problem statement is as follows.

Problem 4 (Quantum Network Tomography of Star Networks). Given a quantum network with star topology T = (V, E), with nodes partitioned into disjoint sets V_E and V_I and channels described by a single Pauli operator as in (4), find an estimator $\hat{\theta}_e$ for the probability vector characterizing \mathcal{E}_e , for all $e \in E$, using measurement statistics from nodes in V_E exclusively.

We describe our methods for pure bit-flip channels and discuss how they generalize to channels described by the other two Pauli operators. Note that we consider the same Pauli operator to describe all channels in the star.

Algorithm 1: Tree state distribution

```
input: tree T; circuit C; function \eta
  output: distributed state \rho(\theta) across r \cup L_T
1 for k \in \{0, 1, \dots, h_{\max}\}:
       for v \in H(k):
           v receives qubit \eta(P_v, v) from P_v;
3
           v performs circuit C_v with received qubit and n_v local qubits in state |0_{n_v}\rangle\langle 0_{n_v}| as input;
4
5
               v sends qubit indexed by \eta(v, u) to u;
6
7
           end
      end
8
9 end
```

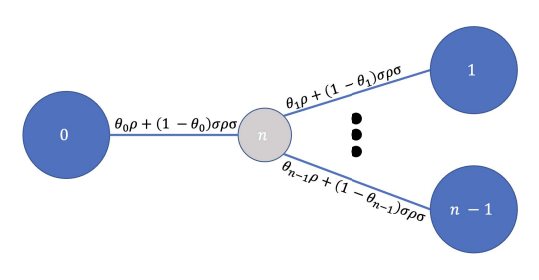


Fig. 2: Star quantum networks with n end-nodes depicted as blue circles. Each channel j in the network is described by a Pauli operator σ and a probability θ_i . The operator-sum representation for the channels is written along the edges of the network.

A. Tomography in the basis of Pauli operators

We start by describing a solution for the tomography in the star that uses states in the Pauli basis. Under the assumption of bit-flip channels, we target states in the Z basis. The same analysis follows for the other single Pauli channels by selecting a different basis according to the Pauli operator under consideration. In the case of Z we use the X basis and in the case of Y we can use either the Z or the X basis.

We are interested in the following distribution process based on Algorithm 1. The root prepares a single qubit in state $|0\rangle$. Since the distribution process assumes that qubits are initialized in state $|0\rangle$, the root applies the identity operator as a circuit, i.e $C_0 = I$. The root transmits the state to the intermediate node, which receives the mixed state

$$\mathcal{E}_0(\rho_n) = \theta_0 |0\rangle\langle 0| + (1 - \theta_0) |1\rangle\langle 1|. \tag{13}$$

The intermediate node applies the generalized Toffoli gate

$$T_n = |0\rangle\langle 0| \otimes I^{\otimes n-1} + |1\rangle\langle 1| \otimes X^{\otimes n-1}$$
 (14)

controlled by the qubit it received on n-1 qubits in its quantum register such that $C(n) = T_{n-1}$, what yields the mixed state

$$\theta_0 |0\rangle\langle 0|^{\otimes n-1} + (1 - \theta_0) |1\rangle\langle 1|^{\otimes n-1}$$
. (15)

The intermediate node assigns its qubits to end-nodes following the order of node labels, such that the qubit indexed by

j is sent to node j+1, with $0 \le j \le (n-2)$. In terms of the inputs of the distribution process, the mapping function selected in the intermediate node is $\eta(n, j + 1) = j$ for $j \in \{0, 1, \dots, n-2\}$. The final mixed state received by the end-nodes is the (n-1)-qubit state

$$\rho(\theta) = \sum_{s \in \mathbb{B}^{n-1}} \alpha(s) |s\rangle\langle s|, \qquad (16)$$

where

$$\alpha(s) = \theta_0 \beta_0(s) + (1 - \theta_0) \beta_1(s), \tag{17}$$

$$\beta_0(s) = \prod_{j=1}^{n-1} \delta_{\overline{s}_j} \theta_j + \delta_{s_j}, (1 - \theta_j),$$

$$\beta_1(s) = \prod_{j=1}^{n-1} \delta_{s_j} \theta_j + \delta_{\overline{s}_j}, (1 - \theta_j),$$

$$(18)$$

$$\beta_1(s) = \prod_{j=1}^{n-1} \delta_{s_j} \theta_j + \delta_{\overline{s}_j}, (1 - \theta_j), \tag{19}$$

 δ_{s_i} is the discrete pulse function equal to 1 if bit $s_j = 1$ and we define $\bar{s}_i = 1 - s_i$. In this case, the final density matrix spans binary strings with n-1 bits and is diagonal on the Zbasis.

We select the POVM to be the set of projective measurements on the Z basis for the Hilbert space of n-1 qubits attained by locally measuring each qubit in the Z basis. Given that local measurements are performed by the end-node, we can write the statistics of flips in each particular bit as follows. Let $S_i \in \{0,1\}$ denote the measurement outcome of the qubit in node j. A bit-flip is measured in node j if a flip occurs exclusively on one of the channels 0 and j. Let $F_i \in \{0,1\}$ denote the absence or presence of a bit flip on channel j. We have $S_j = F_0 \oplus F_j$, where \oplus denotes the XOR operation. Thus, the probability of measuring a bit-flip in qubit j is

$$Pr[S_i = 1] = \theta_0(1 - \theta_i) + (1 - \theta_0)\theta_i, \tag{20}$$

for all $j \in \{1, \dots, n-1\}$. Using (20) for all channels in the star yields a system of n-1 first-order, bi-variate polynomial equations over n variables. However, all of these equations depend on θ_0 and, if θ_0 can be computed, the system reduces to a system of n-1 independent linear equations.

The dependency between S_i and F_0 introduces dependencies between all pairs of variables S_j, S_k for all cases where $\theta_0 \neq 0.5$. This dependency can be exploited to obtain an equation for θ_0 as follows. Let $S_{jk} = S_j S_k$ denote the joint random variable obtained by concatenating S_j and S_k . Also, let $Pr[S_j=1]=p_j$ and $Pr[S_{jk}=11]=p_{jk}$. The probability that any two flips are jointly measured by end-nodes j and k is

$$p_{jk} = \theta_0 (1 - \theta_j)(1 - \theta_k) + (1 - \theta_0)\theta_j \theta_k.$$
 (21)

The probability in (20) can be re-arranged to obtain

$$\theta_j = \frac{p_j - \theta_0}{1 - 2\theta_0},\tag{22}$$

which is valid for all $j \in \{1, 2, ..., n-1\}$. Plugging back on (21) yields the quadratic equation

$$a_{jk}(1 - \theta_0)\theta_0 + c_{jk} = 0 (23)$$

for θ_0 , where

$$a_{jk} = 1 + 4p_{jk} - 2(p_j + p_k),$$
 (24)

$$c_{jk} = p_j p_k - p_{jk}. (25)$$

The form of (23) is symmetric with respect to probabilities since if θ^* solves the equation, $(1-\theta^*)$ also does. This inherent symmetry implies that solving (23) for a specific pair of end-nodes (j,k) determines two possible values for θ_0 that are valid for the measurement results. More interestingly, the symmetry cannot be broken even when considering (23) for all pairs of end-nodes.

Finally, combining the system from (20) with (23) gives two vectors $\hat{\theta}$ for the channel parameters that are compatible with the observations. Following our characterization, the estimators obtained from this method do not identify the parameters completely, since we have two possible values of $\hat{\theta}$. Given the form of the solutions, identifiability can be obtained by assuming either low or high noise regime for θ_0 . In this case, it suffices to select the solution of (23) that is greater than 0.5 in the low noise regime and the smaller one in the high noise regime.

We simulate a four-node star with bit-flip channels characterized by $\theta = [0.8, 0.3, 0.4]$ to demonstrate the estimators using Z basis measurements. We plot the estimated value for the three parameters with respect to the number of measurement outcomes used for estimation in Figure 3. The symmetry in the estimators appears in the form of the two curves obtained for each parameter. The two values obtained for θ are [0.8, 0.3, 0.4] and [0.2, 0.7, 0.6], and identifiability can only be achieved by making an assumption on the error model.

B. Tomography in the GHZ basis

The need to introduce another assumption to obtain identifiability of the parameters motivates the search for other estimators. We now proceed to describe how GHZ states can be used to address this issue. In particular, we define estimators that use global measurements in the end-nodes, which can be attained by pre-sharing entanglement among the end-nodes. One can argue that end-to-end entanglement is an important resource in a quantum network, and using global measurements introduces complexity in the implementation of our tomography process. Nonetheless, it is of interest to the

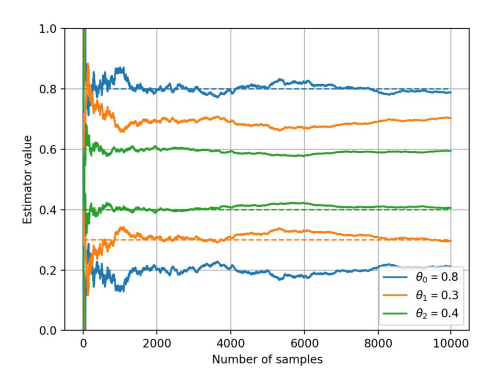


Fig. 3: Estimator using Z basis measurements for a four-node star graph with ground-truth parameter vector $\theta = [0.8, 0.3, 0.4]$. The dotted lines show ground-truth values for the parameters. The estimators cannot identify the parameters and there are two solutions compatible with observations.

scope of this work to analyze the benefits that entanglement may provide in the network tomography setting.

The GHZ basis generalizes the Bell basis to multiple qubits. From (1), n bits are necessary to describe an n-qubit state in the GHZ basis. Such states are maximally entangled and interesting in this scenario because they remain in the GHZ basis after applying Pauli operators. Formally, the state $|\Phi_s^b\rangle$ evolves under the application of a Pauli operator σ on its j-th qubit as

$$\sigma |\Phi_s^b\rangle = \begin{cases} |\Phi_{s \oplus s_j}^b\rangle, & \sigma = X, \\ i|\Phi_{s \oplus s_j}^{b \oplus 1}\rangle, & \sigma = Y, \\ |\Phi_s^{b \oplus 1}\rangle, & \sigma = Z, \end{cases}$$
 (26)

where s_j is a binary string with 1 in position j if j > 0 and string $11 \dots 1$ if j = 0.

The instance of the distribution process used previously to distribute a mixed state diagonal on the Z basis can be modified to distribute a mixed state diagonal on the GHZ basis by simply changing the circuit applied by the root. Instead of sending state $|0\rangle$ to the intermediate node, the root prepares the Bell state $|\Phi_0^0\rangle$ and sends the second qubit to the intermediate node. This is achieved by the circuit $C_0 = [H \otimes I, CNOT]$, assuming that the CNOT gate is controlled by the first argument. When describing circuits with multiple gates, we use an ordered list notation [,] to indicate that gates are applied on the order they appear inside the square brackets. We select the second qubit to be transmitted just to simplify notation because (1) uses the first qubit as the reference binary value in the GHZ state superposition. If this is indeed the only modification considered, the mixed state received by the intermediate node is

$$I \otimes \mathcal{E}_0(\Phi_0^0) = \theta_0 \Phi_0^0 + (1 - \theta_0) \Phi_1^0 \tag{27}$$

and the final mixed state distributed is

$$\rho(\theta) = \sum_{s \in \mathbb{R}^{n-1}} \alpha(s) \Phi_s^0, \tag{28}$$

with probabilities $\alpha(s)$ given by (17).

By comparing (16) and (28), there is no gain when using GHZ states. This is intuitively understood by considering the fact that only n-1 bits of the GHZ state are used to parameterize the necessary information, which is the same amount of bits used in the initial case. Thus, the key to obtain parameter identifiability is to slightly modify the circuit applied by the intermediate node to transform the r.h.s of (27) into the mixed state

$$\theta_0 \Phi_0^0 + (1 - \theta_0) \Phi_0^1 \tag{29}$$

before the intermediate node transmits. Departing from (29), the final mixed state distributed is described by the n-qubit density matrix

$$\rho(\theta) = \sum_{s \in \mathbb{B}^{n-1}} \theta_0 \beta_0(s) \Phi_s^0 + (1 - \theta_0) \beta_1(s) \Phi_s^1, \tag{30}$$

where β_0 and β_1 are given in (18) and (19), respectively.

The implications of (30) for estimation are profound. In particular, assume that the state in (30) is measured in the GHZ basis, yielding the state $|\Phi_s^b\rangle$. A bit-flip occurred in channel 0 if, and only if, b=1, while a flip occurred in channel j>0 if, and only if, $s_j=1$. Thus, we estimate all the parameters in the network by computing the number of times b=1 and $s_j=1$ in the strings obtained from GHZ measurements in a given set of observations.

In order to transform (27) into (29) it is necessary to modify the circuits applied by the root and the intermediate node. The root circuit is incremented by applying the single qubit gate XHX on the qubit that remains in the root after the CNOT, leading to $\mathcal{C}_0 = [H \otimes I, \text{CNOT}, XHX \otimes I]$. For the intermediate node, the circuit is extended with the application of the single qubit gate HZ to the received qubit before using it as the control for the generalized (n-1)-qubit Toffoli gate, which yields $\mathcal{C}_n = [HZ \otimes I^{\otimes n-2}, T_{n-1}]$.

The same circuit can be used to identify parameters for Y channels with a modification on the estimators. When channels are described by Y, the intermediate node receives the state $\theta_0 \Phi_0^0 + (1 - \theta_0) \Phi_1^1$. The estimators must change when such state is transmitted because the phase bit b and the string s determine together the occurrence of flips in the first channel, what occurs iff $b \neq \bigoplus_{j=0}^{n-1} s_j$. Since the occurrence of a flip in \mathcal{E}_0 can always be detected, it is simple to relate s_i to the occurrence of a flip in channel j. For the Z case, it suffices to add the (n-1)-qubit Hadamard gate $H^{\otimes n-1}$ to the intermediate node circuit, such that $C_0 = [H \otimes I, \text{CNOT}, HX \otimes I, H^{\otimes n-1}]$. In addition, the n-1 end-nodes receiving the qubits from the intermediate node must apply a Hadamard gate before measuring in the GHZ basis. In this case, the bits characterizing the measured GHZ state provide direct estimators for the channel parameters as for X channels.

We simulate the same four-node system used in the analysis of Z-basis measurement estimators with the GHZ scheme for the purpose of comparison. The results reported in Figure 4 show that a single, correct value for θ is identified. Moreover, the curves in Figure 4 are smoother than the ones in Figure

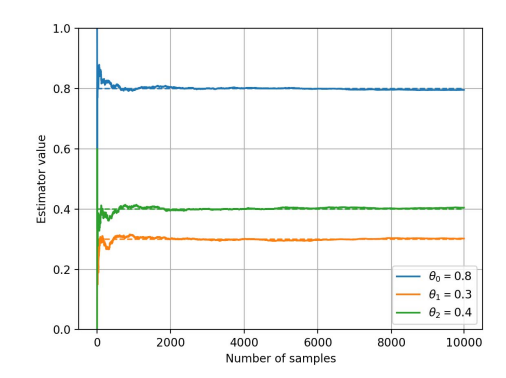


Fig. 4: Estimators based on GHZ measurements for the fournode star graph with ground-truth parameter vector $\theta = [0.8, 0.3, 0.4]$. The estimators identify θ and provide a single solution for the tomography problem. Dotted lines show ground-truth values.

3, indicating that the GHZ-based estimator has less variance than the Z-based one.

C. Estimators and the QCRB

The form of (16) and (30) fits into the definition of Theorem 1, such that the QFIM follows (10) for both estimators. Moreover, we do not explicitly compute the QFIM, although it follows from Theorem 1 that we attain the QCRB in both cases since we use projective measurements on the basis that diagonalize the SLD of all parameters. Finally, the eigenvalues of $\rho(\theta)$ are first-order multivariate polynomials on both scenarios and evaluating (10) for such functions is straightforward, albeit space consuming.

VI. CONCLUSION

The definition of quantum network tomography is key among the main contributions of this work, connecting quantum tomography with classical network tomography. It defines the characterization of links in a quantum network when intermediate nodes do not provide information for estimation. The new problem differs from quantum process tomography on the assumption of a priori knowledge on the form of Kraus operators characterizing network links, while preventing generic measurements for estimation.

We formally described a state distribution process across trees that provides the necessary mixed states for quantum network tomography. The process can be used for trees of arbitrary topology and gives a direct way to address the problem for graphs, since any graph be decomposed into trees. The process was used to solve quantum network tomography in the scenario of star networks with channels described by a single Pauli operator. Our results indicate that entanglement may provide advantages for quantum network tomography. The estimator obtained from global measurements outcomes in the end-nodes identifies the parameters without the need for any additional assumptions, in contrast with the lack of

identifiability observed for local measurements. This evidence motivates the description for the conditions under which entanglement enhances network tomography, as it has been previously investigated for other quantum estimation problems such as quantum sensing networks [23].

We identify four directions for future work. First, solving the tomography problem for star systems with more complex quantum channels, like the depolarizing channel, is key to provide useful tomography methods for real quantum networks. Second, obtaining descriptions for estimators that maximizes the QFIM for star graphs is of interest. Third, solving the problem for generic trees will provide further understanding on the limits of estimation with measurements exclusively at the end-nodes. Finally, framing the optimization problem to characterize the optimal way to partition a network into trees for tomography will bring insights on how the tomography problem generalizes to arbitrary networks.

Acknowledgments—This research was supported in part by the NSF grant CNS-1955744, NSF-ERC Center for Quantum Networks grant EEC-1941583 and by the MURI ARO Grant W911NF2110325.

REFERENCES

- H Jeff Kimble. The quantum internet. *Nature*, 453(7198):1023–1030, 2008.
- [2] Rodney Van Meter. Quantum networking. John Wiley & Sons, 2014.
- [3] Stephanie Wehner, David Elkouss, and Ronald Hanson. Quantum internet: A vision for the road ahead. *Science*, 362(6412), 2018.
- [4] Wojciech Kozlowski and Stephanie Wehner. Towards large-scale quantum networks. In *Proceedings of the Sixth Annual ACM International Conference on Nanoscale Computing and Communication*, NANOCOM '19, New York, NY, USA, 2019. Association for Computing Machinery.
- [5] Robert Beals, Stephen Brierley, Oliver Gray, Aram W Harrow, Samuel Kutin, Noah Linden, Dan Shepherd, and Mark Stather. Efficient distributed quantum computing. Proceedings of the Royal Society A: Mathematical, Physical and Engineering Sciences, 469(2153):20120686, 2013.
- [6] Rodney Van Meter and Simon J Devitt. Local and distributed quantum computation. arXiv preprint arXiv:1605.06951, 2016.
- [7] Charles H Bennett and Gilles Brassard. Quantum cryptography: Public key distribution and coin tossing. arXiv preprint arXiv:2003.06557, 2020.
- [8] Daniel Gottesman, Thomas Jennewein, and Sarah Croke. Longer-baseline telescopes using quantum repeaters. *Physical review letters*, 109(7):070503, 2012.
- [9] Matthew T Rakher, Lijun Ma, Oliver Slattery, Xiao Tang, and Kartik Srinivasan. Quantum transduction of telecommunications-band single photons from a quantum dot by frequency upconversion. *Nature Photonics*, 4(11):786–791, 2010.
- [10] David Awschalom, Karl K. Berggren, Hannes Bernien, Sunil Bhave, Lincoln D. Carr, Paul Davids, Sophia E. Economou, Dirk Englund, Andrei Faraon, Martin Fejer, Saikat Guha, Martin V. Gustafsson, Evelyn Hu, Liang Jiang, Jungsang Kim, Boris Korzh, Prem Kumar, Paul G. Kwiat, Marko Lončar, Mikhail D. Lukin, David A.B. Miller, Christopher Monroe, Sae Woo Nam, Prineha Narang, Jason S. Orcutt, Michael G. Raymer, Amir H. Safavi-Naeini, Maria Spiropulu, Kartik Srinivasan, Shuo Sun, Jelena Vučković, Edo Waks, Ronald Walsworth, Andrew M. Weiner, and Zheshen Zhang. Development of quantum interconnects (quics) for next-generation information technologies. PRX Quantum, 2:017002, Feb 2021.
- [11] Cheng-Zhi Peng, Tao Yang, Xiao-Hui Bao, Jun Zhang, Xian-Min Jin, Fa-Yong Feng, Bin Yang, Jian Yang, Juan Yin, Qiang Zhang, et al. Experimental free-space distribution of entangled photon pairs over 13 km: towards satellite-based global quantum communication. *Physical review letters*, 94(15):150501, 2005.
- [12] Markus Grassl, Linghang Kong, Zhaohui Wei, Zhang-Qi Yin, and Bei Zeng. Quantum error-correcting codes for qudit amplitude damping. *IEEE Transactions on Information Theory*, 64(6):4674–4685, 2018.
- [13] Filip Rozpędek, Thomas Schiet, Le Phuc Thinh, David Elkouss, Andrew C. Doherty, and Stephanie Wehner. Optimizing practical entanglement distillation. *Phys. Rev. A*, 97:062333, Jun 2018.
- [14] Carl W Helstrom. Quantum detection and estimation theory. *Journal of Statistical Physics*, 1(2):231–252, 1969.
- [15] Jing Liu, Haidong Yuan, Xiao-Ming Lu, and Xiaoguang Wang. Quantum fisher information matrix and multiparameter estimation. *Journal of Physics A: Mathematical and Theoretical*, 53(2):023001, 2019.
- [16] G Mauro D'Ariano, Matteo GA Paris, and Massimiliano F Sacchi. Quantum tomography. Advances in Imaging and Electron Physics, 128:206–309, 2003.
- [17] DT Smithey, M Beck, Michael G Raymer, and A Faridani. Measurement of the wigner distribution and the density matrix of a light mode using optical homodyne tomography: Application to squeezed states and the vacuum. *Physical review letters*, 70(9):1244, 1993.
- [18] Quantum-process tomography: Resource analysis of different strategies. Physical Review A, 77(3):032322, 2008.
- [19] Rui Castro, Mark Coates, Gang Liang, Robert Nowak, and Bin Yu. Network tomography: Recent developments. *Statistical Science*, pages 499–517, 2004.
- [20] T. He, L. Ma, A. Swami, and D. Towsley. Network Tomography: Identifiability, Measurement Design, and Network State Inference. Cambridge University Press, 2021.
- [21] F Lo Presti, Nick G Duffield, Joseph Horowitz, and Don Towsley. Multicast-based inference of network-internal delay distributions. IEEE/ACM Transactions On Networking, 10(6):761–775, 2002.
- [22] R. Caceres, N. G. Duffield, J. Horowitz, and D. F. Towsley. Multicast-based inference of network-internal loss characteristics. *IEEE Trans. Inf. Theor.*, 45(7):2462–2480, November 1999.

[23]	Timothy J Proctor, Paul A Knott, and Jacob A Dunningham. parameter estimation in networked quantum sensors. <i>Physical letters</i> , 120(8):080501, 2018.	Multi- review